NAGW 1340
IN-90-CR
211703
P35

Fermi National Accelerator Laboratory

FERMILAB-Pub-89/113A
April 1989

Rate for Annihilation of Galactic Dark Matter into Two Photons

GIAN F. GIUDICE

Fermi National Accelerator Laboratory, Batavia, Illinois 60510

and

KIM GRIEST

Astronomy and Astrophysics Center, Enrico Fermi Institute, The University of Chicago, Chicago, Illinois 60637

and

NASA/Fermilab Astrophysics Center, Fermi National Accelerator Laboratory, Batavia, Illinois 60510

N89-26792
Unclas
G3/90 0211703
(NASA-CR-185029) RATE FOR ANNIHILATION OF GALACTIC DARK MATTER INTO TWO PHOTONS (Fermi National Accelerator Lab.) 35 p CSCL 03B

ABSTRACT

We perform a calculation of the cross section for neutralino-neutralino annihilation into two photons and apply it to dark matter in the galactic halo to find the counting rate in a large gamma ray detector such as EGRET or ASTROGAM. Combining constraints from particle accelerators with the requirement that the neutralinos make up the dark matter we find that rates of over a few dozen events per year are unlikely. We list the assumptions that go into our conclusions and suggest other particle dark matter candidates which could give larger and perhaps observable signals.

Operated by Universities Research Association Inc. under contract with the United States Department of Energy

I. Introduction

It is possible that the dark matter (DM) which exists in the galactic halo consists of some, as yet undiscovered, elementary particle. If this is true and the particle is of the WIMP type (mass greater than 1 GeV and in thermal equilibrium at one time), then the particles may be detectable.[1] Schemes involving direct detection, through DM elastic collisions with nuclei, as well as indirect detection by observing DM particle-antiparticle annihilation products have been discussed and already limits have been placed on some popular DM particle candidates.[1] Since annihilation rates are proportional to the square of the DM number density, the strongest indirect limits have come from annihilation in the body of the Sun or Earth, where large density enhancements are likely, though in these cases it is only the neutrino annihilation products which can be observed.[1]

Detection of antiprotons, positrons and photons from annihilation in the galactic halo has been discussed[1] and found to be difficult; however, interest in photons has been rekindled lately by the suggestion of Bergström and Snellman[2] that annihilation into two photons could give a strong, extremely narrow line (at an energy equal to the mass of the DM particle) which would stand out against the diffuse gamma ray background. In fact, the relevant region of the gamma ray spectrum (> 1 GeV) will be measured for the first time in the very near future by the EGRET instrument on the GRO satellite[3] and larger devices with excellent angular and energy resolution such as ASTROGAM have recently been proposed.[4] The mechanism of Bergström and Snellman is similar to the earlier suggestion of Srednicki, Theisen and Silk[5] that annihilation into charmonium plus photon would give an observable line, but is claimed to take place at a larger rate.

Given the potential importance of the detection of such a line, we thought it worthwhile to check the Bergström and Snellman result, which was found using an approximation, by performing a more complete calculation. We have computed to leading order the gauge invariant set of one-loop box diagrams relevant for the process and find, for photinos or neutralinos, an annihilation

cross section which is more than an order of magnitude *larger* than the Bergström and Snellman result. In the pure photino limit this is in agreement with a very recent calculation of Rudaz,[6] which was done following a different procedure. We also extend the result of Ref. 6 to the more realistic case of a general neutralino (generic combination of photino, zino and higgsino), taking into account the effect of the virtual exchange of possibly light Higgs bosons and charginos. Inclusion of these later particles can give further (but not large) enhancements.

However, even with the enhanced cross section, the counting rate predicted for photino annihilation in a detector such as the GRO EGRET (or even the larger ASTROGAM) is found to quite small, probably less than a few dozen events per year and perhaps below the level of observability. The rate for the general neutralino is for most of the parameter space less than or equal to that for the pure photino special case. These conclusions come about, in part, because accelerator limits on photinos and squarks, in conjunction with limits from photino relic abundance, rule out the regions of parameter space where substantial annihilation would occur. Similar conclusions have been reached (though without the use of accelerator constraints) in a very recent paper by Bouquet, Salati, and Silk[7] who used Rudaz's cross section.

It is important to keep in mind, however, that many different particle models can explain the dark matter and that some of these may evade accelerator bounds and perhaps produce observable signals. We give some examples of such models. In addition, uncertainties in astrophysical quantities such as the density and distribution of dark matter and uncertainties in the particle physics may make observable signals possible.

The plan of this paper is as follows: In Section II we find the cross section by computing explicitly a gauge invariant subset of the contributing Feynman diagrams and expanding our result to leading order in $1/M_{\tilde{f}}^2$ ($M_{\tilde{f}}$ is the mass of the exchanged scalar fermion). The cross section for the generic neutralino (combination of photino, higgsino and zino) is given, though the large enhancement exists only for the photino/zino component. We then use the effective interaction technique to include the effects of chargino and Higgs exchange and discuss the limits of validity of our results.

In Section III we apply the cross section in the photino limit to find the flux in a gamma ray telescope such as ASTROGAM or EGRET. We pick values of the scalar fermion masses consistent with photino dark matter ($.1 \leq \Omega_{\tilde{\gamma}} \leq 1$), and show how this, along with with accelerator constraints from the Fermilab CDF experiment, the SLAC ASP experiment and TRISTAN experiments make rates of more than 40 events per year in the ASTROGAM detector (6 events/year for GRO) unlikely. We also display results for the general neutralino and show how these are in general dominated by the photino component. The Higgs and chargino contributions can be important in some regions of parameter space but in general no large enhancements are to be expected. The diffuse gamma ray background is also briefly discussed.

In Section IV we consider models other than the minimal supersymmetric model. One simple model gives rise to a new dark matter candidate (the "luxino") which would give easily observable fluxes of annihilation gamma rays even in the EGRET detector, while avoiding accelerator constraints and being unobservable via other direct and indirect detection schemes. We point out that the "magnino" of Raby and West[8] would also produce an observable gamma ray line.

In Section V we summarize the paper and make explicit various uncertainties and assumptions contained in our conclusions. We stress the importance of a high resolution gamma ray telescope in resolving some of these issues. Details of the cross section are displayed in the Appendix.

II. Cross Section: $\tilde{\chi}\tilde{\chi} \to \gamma\gamma$

In the minimal supersymmetric model[9] which we consider there are four neutralinos which are linear combinations of the supersymmetric partners of the photon, Z^0, and two neutral Higgs bosons. The lightest of these makes an excellent candidate for the dark matter[10,11,12] and includes the pure photino and pure higgsino as special cases. We denote the lightest neutralino as $\tilde{\chi} = Z_{11}\tilde{B} + Z_{12}\widetilde{W}^3 + Z_{13}\tilde{H}_1 + Z_{14}\tilde{H}_2$, where the Z_{ij} are the elements of the real orthogonal matrix which diagonalizes the neutralino mass matrix. A pure photino has $Z_{11} = \cos\theta_W, Z_{12} = \sin\theta_W$, $Z_{13} = Z_{14} = 0$, while a pure higgsino can have $Z_{11} = Z_{12} = 0$, $Z_{13} = \sin\beta$, and $Z_{14} = \cos\beta$.

The neutralino masses and the Z_{ij}'s are fully determined by four parameters: $\tan\beta$, μ, M, and M', where $\tan\beta \equiv v_2/v_1$ is the ratio of Higgs vacuum expectation values, M and M' are gaugino soft supersymmetry breaking mass parameters, and μ is a supersymmetric Higgs mass. Throughout, we make the standard[9] simplification $M' = \frac{5}{3} M \tan^2\theta_W$. The other relevant free parameters of the supersymmetric model are the masses of the exchanged scalar fermions (squarks and sleptons).

The annihilation into two photons takes place at the one-loop level through diagrams such those of in Fig. 1. (Additional diagrams with exchanged external photon and neutralino legs are not shown, for a total of fourteen diagrams.) Fig. 1 shows a gauge invariant subset consisting of scalar fermion plus fermion exchanges. Additional contributions from Z^0 plus fermion exchange are shown in Fig. 2, and additional contributions coming from chargino and Higgs exchange will be discussed later. As will become apparent when we discuss rates in a gamma ray detector, we are interested in cases where the neutralino is less massive than the weak scale (m_W). We will therefore simplify the calculation by making an expansion in $(m_\chi/m_W)^2$ or $(m_\chi/M_{\tilde{f}})^2$, where $M_{\tilde{f}}$ is the sfermion mass.

First consider the calculation of the amplitude given by the diagrams of Fig. 1. We wrote the fourteen amplitudes for the general neutralino using the Feynman rules given in Refs. 9 and 13, and checked gauge invariance. We then performed the loop integrals after expressing them as three dimensional integrals over Feynman parameters in the standard way. At this point the expression for the total amplitude was quite lengthy and to simplify the calculation (and for the reason given above) we expanded in $1/M_{\tilde{f}}^2$ before evaluating the Feynman parameter integrals. The exception was the diagram of Fig. 1d, where the integrand has a singular expansion in $1/M_{\tilde{f}}^2$. Here we explicitly evaluated the parametric integrals and then made the expansion, a rather lengthy calculation. Collecting terms and using several gamma matrix identities we found that all the gauge non-invariant pieces canceled and have a simple and gauge invariant expression for the amplitude

$$\mathcal{M} = \frac{8\alpha^2 m_\chi}{\sin^2\theta_W s}\epsilon^{\mu\nu\rho\sigma}k_{1\mu}k_{2\nu}\epsilon_{1\rho}\epsilon_{2\sigma}\bar{v}(p_2)\gamma_5 u(p_1)\frac{c_i Q_i^2}{M_{\tilde{f}i}^2}\left(1-\frac{4m_i^2}{s}I\left(\frac{\sqrt{s}}{2m_i}\right)\right) \times \left(Z_{11}\tan\theta_W(Q_i - T_i^{3L}) + Z_{12}T_i^{3L}\right)^2, \quad (1)$$

where p_1, p_2 (k_1, k_2) are the four-momenta of the neutralinos (photons), ϵ_1 and ϵ_2 are the photon polarizations, m_i, Q_i, and T_i^{3L} are the mass, charge and third component of weak isospin ($\pm\frac{1}{2}$ for doublets and 0 for singlets) of the fermion in the loop, s is the Mandelstam variable, m_χ is the mass of the neutralino, and

$$I(x) = \begin{cases} (\arcsin x)^2 & |x| < 1 \\ \left(\frac{\pi}{2} + i\log(|x| + \sqrt{x^2+1})\right)^2 & |x| > 1. \end{cases} \quad (2)$$

Squaring this and taking the extreme non-relativistic limit valid here (the relative velocity, $v_{\rm rel}$, is about 10^{-3} for galactic dark matter) we can write the resulting cross section for neutralino annihilation into two photons as

$$\sigma v_{\rm rel} = \frac{\alpha^2 G_F^2 {m_\chi}^2}{2\pi^3}\left|\sum_i c_i Q_i^2\left[A_i\left(1-\frac{I(x_i)}{x_i^2}\right) - B_i\frac{I(x_i)}{x_i}\right]\right|^2, \quad (3)$$

where G_F is the Fermi constant, α is the fine structure constant, c_i is a color factor (3 for quarks, 1 for leptons), $x_i = m_\chi/m_i$, and for the fermion plus sfermion exchanges considered in Fig. 1:

$$A_i^{\tilde{f}} = \frac{2m_W^2}{M_{\tilde{f}i}^2}\left(Z_{11}\tan\theta_W(Q_i - T_i^{3L}) + Z_{12}T_i^{3L}\right)^2$$
$$B_i^{\tilde{f}} = 0. \quad (4)$$

It is important to note that the sum must be taken over **both left and right** chiral fermions. This allows the formula to be used with non-degenerate left and right sfermions. Also note that m_χ in eq. (3) carries the sign of the neutralino mass eigenvalue.

We have written the cross section, eq. (3), in this general form so that the contributions from Z^0 exchange as well as chargino and Higgs exchange can be included by just extending the sum to new objects. For example, the Z^0 exchange diagrams of Fig. 2 give a contribution

$$A_i^Z = (Z_{14}^2 - Z_{13}^2)^2 T_i^{3L} \left(\frac{m_Z^2 - 4m_\chi{}^2}{m_Z^2 - 4m_\chi{}^2 - i\Gamma_Z m_Z} \right) \qquad (5)$$
$$B_i^Z = 0,$$

where $\Gamma_Z \approx 2.5$ GeV is the width of the Z^0 and in this case the sum over the right chiral fermions gives zero. The contribution of the diagram of Fig. 2 where the fermion loop is replaced by a loop of $W^\pm$ bosons or squarks and sleptons will be neglected since it does not contribute to leading order in $1/m_W^2$ or $1/M_{\tilde{f}}^2$.

In the pure photino limit, eq. (3) reduces to

$$\sigma v_{\rm rel} = \frac{\alpha^4}{\pi} m_\chi{}^2 \left| \sum_i \frac{Q_i^4 c_i}{M_{\tilde{f}i}^2} (1 - \frac{I(x_i)}{x_i^2}) \right|^2 . \qquad (6)$$

(Note the sum is over both left and right sfermions, which gives a factor of four if they are degenerate.) A pure higgsino limit can also easily be obtained. Bergström, *et al.*,[2] give a formula similar to eq. (6) with $I(x)/x_i^2$ instead of $(1 - I(x)/x_i^2)$. Eq. (6) is in agreement with the recent result of Rudaz,[6] and as shown by him is more than an order of magnitude larger than the earlier estimate of Bergström, *et al.*.

Both the results of Ref. 2 and Ref. 6 were derived by using an effective interaction Lagrangian and computing the triangular fermion anomaly diagram. The disagreement comes from the way gauge invariance was imposed. Here, we took a slightly different and unambiguous approach. We performed the loop integrals of the box diagrams of Fig. 1, where no anomaly is present, explicitly retaining gauge invariance throughout. To leading order in the $1/M_{\tilde{f}}^2$ expansion, the two procedures should give the same result, if performed correctly. In fact, only the diagram of Fig. 1d (plus similar ones with exchanged external legs) can

give rise to a gauge invariant amplitude of order $1/M_{\tilde{f}}^2$. This can be understood by a dimensional argument and by noting that a gauge invariant amplitude must be at least quadratic in the external momenta, since the photons can appear in the effective interaction only through their field strength. Having shown now that the (much simpler) procedure of Rudaz leads to the correct answer, we can include the additional chargino diagrams using his method.

In the minimal supersymmetric model there are two charginos, the supersymmetric partners of the $W^\pm$ and charged Higgs bosons, one of which is always heavier than the $W^\pm$ (and therefore contributes only to higher order in our expansion). Their masses and mixing angles are determined by the parameters $\tan\beta$, M, and μ, defined earlier, and the lightest one can make an important contribution to our amplitude. Replacing the sfermion–fermion–neutralino vertex with the $W^\pm$–chargino–neutralino vertex (see Refs. 9 and 13 for the Feynman rules) we find a chargino plus $W^\pm$ contribution given by the diagrams of Fig. 1, with the $W^\pm$ and chargino taking the places of the sfermions and fermions. As shown in the Appendix, the chargino plus $W^\pm$ contribution adds another term to the sum in eq. (3):

$$\begin{aligned} A^W_{\tilde{\chi}(+)} &= -2(O_L^2 + O_R^2) \\ B^W_{\tilde{\chi}(+)} &= -8O_L O_R, \end{aligned} \tag{7}$$

where $O_L = -Z_{14}V_{12}/\sqrt{2} + Z_{12}V_{11}$, $O_R = Z_{13}U_{12}/\sqrt{2} + Z_{12}U_{11}$, and the U_{ij} and V_{ij} are the matrices which diagonalize the chargino mass matrices (see Ref. 9 appendices). When using eq. (7) in eq. (3), $m_i = m_{\chi(+)}$ and the color factor and charge are unity.

A diagram similar to Fig. 2 with the fermions in the loop replaced by the lightest chargino likewise contributes:

$$\begin{aligned} A^Z_{\tilde{\chi}(+)} &= \frac{1}{2}(Z_{14}^2 - Z_{13}^2)(U_{12}^2 - V_{12}^2)\left(\frac{m_Z^2 - 4m_\chi{}^2}{m_Z^2 - 4m_\chi{}^2 - i\Gamma_Z m_Z}\right) \\ B^Z_{\tilde{\chi}(+)} &= 0. \end{aligned} \tag{8}$$

Finally we consider the exchange of Higgs bosons. There are two scalar Higgs bosons, one pseudoscalar Higgs and two charged Higgs' in the minimal

supersymmetric model. The scalar Higgs contribution vanishes in the extreme non-relativistic limit relevant here, and the charged Higgs' contributions are small since they are heavier than the $W^{\pm}$. The pseudoscalar Higgs contributes via diagrams similar to those of Fig. 2 with the Z^0 replaced by the Higgs boson. For the pseudoscalar Higgs plus fermion exchange we have

$$\begin{aligned} A_i^H &= 0 \\ B_i^H &= 2\frac{m_i m_W}{m_H^2 - 4m_\chi{}^2}(Z_{11}\tan\theta_W - Z_{12})(Z_{14}\cos\beta - Z_{13}\sin\beta)r_i, \end{aligned} \tag{9}$$

where $r_i = \cot\beta$ for up type fermions and $r_i = \tan\beta$ for down type. We have included an extra factor of 2 in eq. (9) so that the sum i may be taken over the fermions only once (previously it had to be taken over both left and right chiral fermions). For the light chargino plus Higgs we also have a contribution:

$$\begin{aligned} A_{\tilde{\chi}(+)}^H &= 0 \\ B_{\tilde{\chi}(+)}^H &= -\frac{2\sqrt{2}m_W^2}{m_H^2 - 4m_\chi{}^2}(Z_{11}\tan\theta_W - Z_{12})(Z_{14}\cos\beta - Z_{13}\sin\beta)(U_{11}V_{12}\cos\beta \\ &\qquad + U_{12}V_{11}\sin\beta). \end{aligned} \tag{10}$$

In the case of pseudoscalar Higgs boson exchange there are no loops of $W^{\pm}$ bosons or squarks and sleptons, so eqs. (10) and (9) give the complete result.

It is important to note that our formulas are valid only in the limit $m_\chi \ll m_W, M_{\tilde{f}}$. Given, as shown in the next section, the low detection rates predicted for heavier neutralinos we feel that at this time the complete result would not be worth the effort and so we content ourselves with displaying results for $m_\chi < 40$ GeV. While heavier neutralinos may well make up the dark matter, it seems unlikely that they will be detectable via their gamma ray lines in the next few years. This concludes our discussion of the cross section.

III. Rate in a Detector

For a spherical isothermal galactic halo of core radius a, and a local dark

matter density $\rho_{\rm halo}$ the flux in a gamma ray detector can be written[14,15]

$$\frac{d\phi}{d\Omega} = {\rho_{\rm halo}}^2 \frac{2\langle\sigma v\rangle_{\rm ann}}{8\pi {m_\chi}^2} \frac{a(1+\alpha^2)^2}{\beta^3} J(b,l), \tag{11}$$

where $\alpha = r_0/a$, r_0 is the distance of the Sun from the galactic center, $\beta = (1+\alpha^2+\alpha^2\cos^2 b\cos^2 l)^{1/2}$, $J(b,l)$ is an integral along the line of sight as a function of the galactic coordinates b and l, and we have included a factor of two for the two photons produced in each annihilation. We consider only high galactic latitudes ($b = \pi/2$) where $J \approx \pi/2$.

Using[1] $r_0 \approx 8.5$ kpc, $a \approx 5.6$ kpc, $\rho_{\rm halo} \approx .3$ GeV/cm^3 and measuring $\langle\sigma v\rangle$ in units of 10^{-26}cm^3/sec, this becomes

$$\frac{d\phi}{d\Omega} \approx \frac{110\langle\sigma v\rangle_{26}}{(m_\chi/{\rm GeV})^2} \frac{\rm events}{\rm year\ sr\ cm^2}. \tag{12}$$

For EGRET[3] with an effective area/field of view of 900 cm^2 sr this gives

$$R_{\rm GRO} \approx \frac{1.0\times 10^5\langle\sigma v\rangle_{26}}{(m_\chi/{\rm GeV})^2} \frac{\rm events}{\rm year}, \tag{13}$$

while ASTROGAM,[4] with an effective area/field of view of 7000 cm^2 sr gives a rate ≈ 7.8 times larger. We should point out that there is great uncertainty in the astrophysical parameters a, r_0 and especially $\rho_{\rm halo}$ which enter into eq. (11), and that in addition, the halo is probably not an isothermal sphere. Taken together an order of magnitude uncertainty in the rate is probable.

First consider pure photino dark matter. In order to evaluate eq. (13) using eq. (6) we need to choose values of the slepton and squark masses. These are free parameters of the minimal supersymmetric model most often considered, but fortunately the requirement that the relic abundance of photinos be consistent with the photino's role as galactic dark matter constrains the masses considerably. If we require $0.1 \le \Omega_{\tilde\gamma} \le 1$, where $\Omega_{\tilde\gamma}$ is the ratio of the average photino density in the Universe to the critical density, and choose the value of the Hubble parameter $h = 1/2$, (50 km/sec/Mpc), only a fairly narrow range of sfermion masses is allowed.

In Fig. 3a we plot the values of the sfermion masses needed for $\Omega_{\tilde{\gamma}}h^2 = 0.25$ (solid and short dashed lines), while in Fig. 3b we show the same for $\Omega_{\tilde{\gamma}}h^2 = 0.025$. For the lines labeled "not split" we assumed that all squarks and sleptons (selectron, smuon, stau are the relevant sleptons) have a common mass $M_{\tilde{f}}$. For the lines labeled "split" we took a common squark mass, $M_{\tilde{q}}$, and a common slepton mass, $M_{\tilde{e}}$, but assumed $M_{\tilde{e}} = M_{\tilde{q}}/3$. This is theoretically more attractive than the degenerate case.[16] The slepton masses are labeled ($\tilde{e}$) (for selectron) and are nearly the same as the common sfermion masses in the "not split" cases. This is to be expected since annihilation is dominated by the exchange of the lightest sfermion allowed. This will become important when we consider accelerator limits on the supersymmetric particles.

The values of the sfermion masses, (and therefore the two-photon cross sections) are found by requiring the indicated value of $\Omega_{\tilde{\gamma}}h^2$ for each value of the photino mass $m_{\tilde{\gamma}}$. For each value of $m_{\tilde{\gamma}}$ we solve the Boltzmann equation which determines the relic abundance of photinos as they annihilated in the early universe. We use an approximate, but very accurate (better than 5%) method which takes into account propagator momenta in the $\tilde{\gamma}\tilde{\gamma} \to q\bar{q}$ cross sections as well as the changing degrees of freedom as the universe cools. See Refs. 17 and 11 for details of the method, cross sections and references.

Using the sfermion masses from Fig. 3, we plot the counting rate from halo annihilation of pure photinos for the ASTROGAM detector in Fig. 4 and for GRO's EGRET device in Fig. 5. Rates for both the split and degenerate cases are shown, although very little difference in the rates results. (Again, the rate is dominated by the lightest sfermions, *i.e.* the sleptons, and the Q_i^8 factor also favors the sleptons since they have unit charge.)

For reference we also show a possible background rate as estimated by Stecker and Tylka.[18] The background rate is problematic since there are no measurements available at the relevant energies. Extrapolation from the 100 MeV region, where measurements have been made, seems unlikely to be accurate, and one therefore must rely upon theoretical calculations. The main source is thought to be photons from π^0 decay,[18] where the pions are produced in cosmic ray interactions with the interstellar medium. A significant extragalactic component may (or may

not) exist and the background may be much lower in directions which have a low column density of ISM. We therefore consider the background estimates to be extremely uncertain. We simply integrate Stecker and Tylka's estimate over the instrumental field of view and plot the number of events expected in an energy bin the size of the detector resolution (15% for EGRET,[3] and 1% for ASTROGAM[4]). The actual background could differ significantly from this when it is measured. See Refs. 7 and 18 for a more complete and careful discussion of background and how to extract a signal from it.

More important at this point than the uncertain background is the low counting rates seen in Figs. 4 and 5. For the lowest value of $\Omega_{\tilde{\gamma}}h^2$ we consider (Fig. 4b), photinos of low mass do give substantial rates, hundreds of events per year being possible. Unfortunately, more careful examination of the squark and/or slepton masses required to produce this low $\Omega_{\tilde{\gamma}}h^2$ shows that photinos with masses less than around 11 GeV are inconsistent with either CDF or ASP experimental results.

This is shown in Fig. 3b where one long-dash line shows the CDF limit[19] $M_{\tilde{q}} \leq 74$ GeV (90% c.l.) and the other long-dash line shows the ASP limit[20] on the photino/selectron masses. The ASP line was found using $\sigma(e^+e^- \rightarrow \tilde{\gamma}\tilde{\gamma}\gamma) < 0.03$ pb, and the relevant experimental acceptance. See Ref. 11 for the cross sections used, more details and further references. The TRISTAN[21] limit ($M_{\tilde{e}} > 26$ GeV) does not further constrain the parameter space.

Fig. 3b shows that for the case of degenerate squarks and sleptons (not split), the squark mass always falls below the CDF limit, ruling this case out. For the $M_{\tilde{e}} = M_{\tilde{q}}/3$ (split) case, the squark masses evade the CDF limit for photinos above around 3 GeV in mass, but the selectrons fall below the ASP limits for photinos below around 11 GeV. Taken together we see that for the $\Omega_{\tilde{\gamma}}h^2 = .025$ case, photinos lighter than around 11 GeV are ruled out, independent of squark/slepton splitting. Referring back to Fig. 4b we conclude that a rate larger than around 40 events per year in ASTROGAM is unlikely. We should also point out that for $m_{\tilde{\gamma}} > 70$ GeV, the squark/slepton masses necessary for $\Omega_{\tilde{\gamma}}h^2 = .025$ are less than $m_{\tilde{\gamma}}$. This is inconsistent with our assumption of photino dark matter since only the lightest supersymmetric particle is expected to be stable. However,

as mentioned previously, the expansion used in calculation of the cross section breaks down before this and so we do not display these cases anyway.

Fig. 3a shows that the limits from CDF and ASP for the $\Omega_{\tilde{\gamma}}h^2 = .25$ case are much less stringent. For the degenerate case CDF allows photinos heavier than 9 or 10 GeV, while for the split case photinos heavier than 2 GeV are allowed by CDF. The combined CDF and ASP limits allow photinos heavier than around 5 GeV. However, Fig. 4a shows that the rates for the $\Omega_{\tilde{\gamma}}h^2 = .25$ case are correspondingly lower (for the same reason!), and again it seems that rates above a few events per year in ASTROGAM are unlikely.

As shown in Fig. 5, the rates expected in the soon to be launched GRO EGRET detector are substantially lower (and the background is higher), with less than 10 events per year expected if $\Omega_{\tilde{\gamma}}h^2 = .025$ and less than 1 per year if $\Omega_{\tilde{\gamma}}h^2 = .25$.

We should mention, at this point, that a way to evade the crucial ASP limit without lowering the photon event rate is to have a heavy selectron in conjunction with a light smuon or stau. The ASP cross section depends only on the selectron mass and therefore limits only this mass. However, while one may reasonably expect the colored squarks to split from the uncolored sleptons and even the stop squark to split from the other squarks due to the large top mass, there is no ready mechanism to split the sleptons among themselves, the electron, muon and tau have identical quantum numbers are are all relatively light, so we consider this possibility unlikely.

Up to now we have considered only the pure photino special case of the neutralino, and only sfermion/fermion particles in the loops. This case is simple to display because the sfermion masses and rate are determined by the photino mass. For the generic neutralino there are more parameters (namely $\tan\beta$, μ and M, as discussed in Sec. II). However, we will now show that the simple case already displayed is very likely a rough upper limit to the rates possible for the generic neutralino.

In Fig. 6 we show expected rates in the ASTROGAM detector for a set of supersymmetric parameters consistent with $\Omega_{\tilde{\chi}}h^2 = .025$. For comparison, we

plot (solid line) the rate for a pure photino from Fig. 4b (split case). All the points (x's and boxes) are models with $M_{\tilde{q}} = 120$ GeV and $M_{\tilde{e}} = 40$ GeV, and therefore correspond in the pure photino limit to a single point on the solid line (near the big "blob"). The points are found by taking the above sfermion masses and values of $\tan\beta$ of 5, 2, 1.1, and .25, and then solving for all points (on a grid) in the μ, M plane which satisfy $\Omega_{\tilde{\chi}}h^2 = .025$. Values of M and $|\mu|$ from 0 to 1 TeV are considered, the x's showing positive values of μ and the boxes negative values.

To imagine the effect of including all of supersymmetric parameter space first fill in the area between all the points. This takes into account all values of $\tan\beta$, μ and M. Then "slide" the pure photino "blob" and attached filled area along the solid line, thus taking into account all possible values of squark masses. Note that the "blob" is the projection of the many points in supersymmetric parameter space which have large photino components.

It is clear from Fig. 6 that the rate for the general neutralino seldom rises above the rate for a pure photino. This is to be expected since eq. (3) shows that any higgsino component is heavily suppressed with respect to any photino component, and the zino component is of the same order as the photino component. One might expect the chargino contribution (which is included in Fig. 6) to enhance the rate, since it can be very light. However, experimental searches at TRISTAN[21] have ruled out charginos of mass less than 26 GeV and we therefore include only models (parameter values) which predict $m_{\chi(+)} > 26$ GeV. Even apart from this, the chargino is really just another fermion in the loops of Figs. 1 and 2, and since only one chargino is relevant, and it has no color factor, it cannot be expected to overwhelm the contributions from the many quarks and leptons. The small mass of the selectron (40 GeV) also enhances the effect of the sfermion exchange diagrams over the chargino exchange. In fact, for lower values of $\Omega_{\tilde{\chi}}h^2$, where larger sfermion masses are required, the role of the chargino is much more important (but the rates in a detector are smaller). It is interesting to note that one important effect of the chargino is to increase the rate for the pure higgsino case, which is usually thought to be quite suppressed.

Next, we discuss the effects of the pseudoscalar Higgs boson. We have not

included the contributions from the Higgs in Fig. 6, even though it can be very light. A light Higgs might be thought to give a large enhancement due to the propagator $(m_H^2 - 4m_\chi{}^2)^{-2}$. However, the $4m_\chi{}^2$ term dominates for light Higgs', and except near the pole, the additional factor of $(m_i/m_W)^2$ and the fact that the selectron mass is so low, makes the Higgs contribution small in comparison for the case under consideration. We did investigate numerically the effect of a light Higgs, finding that a substantial enhancement is present only close to the resonance. However, in these circumstances one expects neutralino annihilation in the early universe to be more efficient, diluting the relic density proportionally. Note that again, for lower $\Omega_{\tilde{\chi}} h^2$, the Higgs contribution can be dominant, but again the rates in a detector are small.

Finally, we point out that inclusion of the chargino and Higgs contributions, along with consideration of the general neutralino, make the very low rates expected for the pure higgsino not nearly as likely. Detection of the general neutralino is most likely easier than detection of a pure higgsino. Due to the low rates, however, a full exploration of the supersymmetric parameter space will not be conducted at this time; rather we will explore other models which have the potential for giving large and probably observable signals.

IV. Models with Large Rates

In this section we attempt to find particle models which evade existing particle accelerator constraints and give large gamma ray signals. The counting rate in a gamma ray detector from DM annihilation is low primarily for two reasons. First, the number density of DM particles in the halo is low, and the annihilation rate is proportional to the density squared. Second, the cross section for annihilation of neutral particles into two photons typically occurs only at the loop level, implying that the annihilation cross section is low. Now the total annihilation cross section of a candidate DM particle can be determined (at "freeze-out") by requiring a cosmologically relevant relic abundance

$$\langle \sigma v \rangle_{ann} \sim \frac{10^{-26}}{\Omega h^2} \frac{\mathrm{cm}^3}{\mathrm{sec}}, \tag{14}$$

where some dependence upon the "p" vs. "s" wave annihilation has been left

out. The problem with the neutralino (and massive neutrino, etc.) is that the annihilation cross section which eq. (14) determines is dominated by the quark-antiquark and lepton-antilepton channels, leaving the two photon cross section smaller by factors of α^2/π^2. As a way around this, we consider a class of particles (called "*luxinos*", for "lux": light) whose main annihilation channel in the early universe is into photons. Assuming this, eqs. (13) and (14) predict

$$R_{\rm GRO} \approx \frac{10^5 (m_l/{\rm GeV})^{-2}}{\Omega_l h^2} \frac{\rm events}{\rm year}, \tag{15}$$

and a rate about eight times larger for ASTROGAM. Here m_l and Ω_l are the luxino mass and relic energy. This substantial rate would be easily visible above background by the EGRET detector.

As an existence proof that such particles are possible, consider a model with a neutral Majorana fermion luxino l^0, a pair of charged fermions $l^\pm$ and a neutral scalar ϕ. Assuming the l^0 is a singlet under the standard model gauge group, we introduce the interaction Lagrangian

$$\mathcal{L}_l = \bar{l}^0 (a + b\gamma_5) l^0 \phi + \bar{l}^\pm (a' + b'\gamma_5) l^\pm \phi + {\rm h.c.}. \tag{16}$$

For simplicity, we will consider the case where $l^\pm$ and ϕ have a common mass M (larger than the luxino mass m_l). The luxino annihilates through the diagrams of Fig. 7 leading in the non-relativistic limit to the cross section

$$\sigma(l^0 l^0 \to \gamma\gamma) v \approx \frac{4\alpha^2 m_l^4}{\pi^3 M^6} b^2 \left(\frac{4}{9} a'^2 + b'^2\right), \tag{17}$$

where we have taken $M \gg m_l$. The other channels, $l^0 l^0 \to (\gamma^*, Z^*) \to \bar{f} f$ are not able to compete with $l^0 l^0 \to \gamma\gamma$, since l^0 develops non-vanishing electroweak form factors only at the two loop level. This also implies that the luxino has a very feeble electroweak coupling with ordinary matter, which makes it invisible in direct dark matter detection experiments via nuclear recoil. If we take the

coupling constants b, a' and b' to be of order unity, the present luxino density is given roughly by

$$\Omega_l h^2 \approx 8 \times 10^{-5} \frac{(M/\mathrm{GeV})^6}{(m_l/\mathrm{GeV})^4}. \tag{18}$$

Dark matter luxinos in the mass range of 10 to 50 GeV require M in the range 25 to 70 GeV. In order to make the model complete, we need to add to the Lagrangian, eq. (16) some interactions able to mediate the decay of the charged $l^{\pm}$ particles. One possibility is to introduce heavy (> TeV) charged scalars or gauge bosons which couple a $l^{\pm}$–l^0 pair to ordinary fermions (f) and allow the process $l^{\pm} \to l^0 f f'$.

This example illustrates a particle which predicts a photon counting rate as large as eq. (15), but which is invisible in other accelerator and dark matter search schemes.

Finally, we want to mention that large monochromatic gamma ray production can be expected in the model of the magnino, proposed in Ref. 8 to solve the solar neutrino and dark matter problems. In this model, the spin $\frac{1}{2}$ neutral magnino (m^0) has a Yukawa interaction with a charged fermion m^+ and a Higgs scalar h^+. The masses of m^+ and h^+ are almost degenerate with the magnino mass in order to provide it with a large magnetic moment and still escape experimental detection. The annihilation $\bar{m}^0 m \to \gamma\gamma$ occurs through the diagrams of Fig. 1 (substituting m^+ and h^+ in the internal lines). In the non-relativistic limit, we obtain a cross section of order

$$\sigma(\bar{m}^0 m^0 \to \gamma\gamma)v \sim \frac{\alpha^2 g^4}{8\pi^3 m_0^2}, \tag{19}$$

where g is the Yukawa coupling of order unity, and m_0 is the magnino mass, which must be in the range 5 to 10 GeV to solve the solar neutrino problem. Taking into account that, in order to solve the solar neutrino problem, the number density of anti-magninos must be less than the number density of magninos by a factor

of two or so, we obtain a maximum counting rate for the EGRET detector of

$$R_{\rm GRO} \sim 5 \times 10^5 (m_0/5\ {\rm GeV})^{-2} \frac{\rm events}{\rm year}. \qquad (20)$$

It is important to recall, however, that a recent reanalysis[22] of the e^+e^- annihilation data from the Mark II detector at SLAC has left only a very narrow allowed region for the magnino mass parameters and the model seems disfavored.

V. Conclusions and Discussion

We have performed a careful calculation of the cross section for the annihilation of galactic neutralinos into two photons and shown that the rate of annihilation can be substantial, mainly due to the gaugino (photino and zino) component, dominating the rate into charmonium plus photon.[5] Two[2,6] calculations of the this cross section differ by more than an order of magnitude and we have shown using a different procedure that the enhanced results of Rudaz are correct to first order in $M_{\tilde{f}}^{-2}$. We have included the effects of charginos and Higgs bosons in the loop diagrams and shown that while they can make important contributions, no further large enhancements are to be expected.

Even with this greatly enhanced cross section, however, we find for canonical values of the galactic halo parameters, that less than a few dozen events per year will be seen in a gamma ray detector the size of ASTROGAM. This is due, in large part, to the constraints put on dark matter photinos by accelerator results from the CDF and ASP experiments.

To see if other dark matter candidates might produce more interesting gamma ray signals we then introduced a new class of models (the "luxinos") whose main annihilation channel is two photons. These can give much larger, probably observable signals. We pointed out that the magnino of Raby and West[8] can also provide large signals.

Since the data available on the identity of the dark matter is so scarce, it is important that high resolution gamma ray searches take place. These will complement the direct detection experiments and the search for annihilation

neutrinos in proton decay detectors. While we did not emphasize background, we should note that the intrinsic width of the gamma ray line is $\sim 10^{-3}$ and that a detector with an energy resolution of 10^{-3} could cut the background by a factor of 100 over ASTROGAM. It is also the case that uncertainties in the distribution and density of dark matter could increase the rate substantially over our estimates. This is especially true if there is a large concentration of dark matter near the galactic center.[23]

Finally we should note that our neutralino results are only valid to first order in $m_\chi/M_{\tilde{f}}$ and that above around 40 GeV they are not to be trusted. While it is certainly possible that neutralinos more massive than this make up the dark matter, the photon counting rate is dropping rapidly and the substantial increase in cross section that would be needed to allow easy observation of these heavy neutralinos seems unlikely.

In conclusion, we feel that while the outlook for neutralino detection in the near future via halo annihilation is rather pessimistic, the uncertainties in the predictions are large enough to warrant a careful search for sharp lines in the diffuse gamma ray background.

Acknowledgements

We would like to acknowledge very useful conversations with L. Hall, D. Kniffen, S. Rudaz, D. Seckel, F. Stecker and M. Ulmer. This work was supported in part by the DoE (at Chicago) and the DoE and NASA (grant NAGW-1340) (at Fermilab).

Appendix

In this appendix we derive the A_i and B_i functions of eq. (3) using the effective interaction technique of ref. 6. The effective Lagrangian, valid for $M_{\tilde{f}}, m_W \gg m_\chi$, for the interaction between neutralinos and fermions (quarks or leptons) is

$$\mathcal{L}^f_{eff} = \sqrt{2} G_F \chi\gamma^\mu\gamma_5\chi \; \bar{f}\gamma_\mu(\alpha_L P_L + \alpha_R P_R) f, \qquad (A1)$$

where

$$\begin{aligned}
\alpha_L =&(Z_{14}^2 - Z_{13}^2)(Q_f \sin^2\theta_W - T_f^{3L}) - 2\frac{m_W^2}{M_{\tilde{f}L}^2}\left[Z_{11}\tan\theta_W(Q_f - T_f^{3L}) + Z_{12}T_f^{3L}\right]^2 \\
\alpha_R =&(Z_{14}^2 - Z_{13}^2)Q_f \sin^2\theta_W + \frac{2m_W^2}{M_{\tilde{f}R}^2}(Z_{11}\tan\theta_W Q_f)^2,
\end{aligned} \tag{A2}$$

$P_L = (1-\gamma_5)/2$, $P_R = (1+\gamma_5)/2$, and all other symbols were defined in Sec. II.

For the neutralino–chargino interaction we have

$$\begin{aligned}
\mathcal{L}_{eff}^{\tilde{\chi}^{(+)}} = \sqrt{2}G_F\Big[&\bar{\chi}\gamma^\mu\gamma_5\chi\ \bar{\chi}^{(+)}\gamma_\mu(\beta_L P_L + \beta_R P_R)\chi^{(+)} \\
&+ \beta_5\left(\bar{\chi}\chi\ \bar{\chi}^{(+)}\chi^{(+)} + \bar{\chi}\gamma_5\chi\ \bar{\chi}^{(+)}\gamma_5\chi^{(+)}\right)\Big],
\end{aligned} \tag{A3}$$

where

$$\begin{aligned}
\beta_L =&(Z_{14}^2 - Z_{13}^2)\left(-1 + \sin^2\theta_W + \frac{1}{2}V_{12}^2\right) + 2O_L^2 \\
\beta_R =&(Z_{14}^2 - Z_{13}^2)\left(-1 + \sin^2\theta_W + \frac{1}{2}U_{12}^2\right) - 2O_R^2 \\
\beta_5 =&4O_L O_R,
\end{aligned} \tag{A4}$$

and O_L and O_R were defined just after eq. (7).

The coupling of the neutralino current to the quark/lepton and chargino currents leads to an effective interaction between the two neutralinos and a pair of photons through the diagrams of Figs. 8. For a fermionic current $\bar{f}\Lambda f$, where $\Lambda = 1$, γ_5, γ_λ, $\gamma_\lambda\gamma_5$ for scalar, pseudoscalar, vector and axial vector couplings respectively, the effective Feynman rules for the triangular loop diagrams of Fig. 8

are

$$\begin{aligned}
\text{scalar} &= i\left(g^{\mu\nu} - \frac{k_1^\nu k_2^\mu}{(k_1 k_2)}\right)\epsilon_{1\mu}\epsilon_{2\nu}\frac{2\alpha}{\pi}\sum_i Q_i^2 c_i m_i[1+(1-\frac{1}{x_i^2})I(x_i)] \\
\text{pseudoscalar} &= \epsilon^{\mu\nu\rho\sigma}k_{1\mu}k_{2\nu}\epsilon_{1\rho}\epsilon_{2\sigma}\frac{2\alpha}{\pi}\sum_i Q_i^2 c_i m_i I(x_i) \\
\text{vector} &= 0 \\
\text{axial vector} &= -\epsilon^{\mu\nu\rho\sigma}k_{1\mu}k_{2\nu}\epsilon_{1\rho}\epsilon_{2\sigma}(k_1+k_2)_\lambda\frac{\alpha}{\pi}\sum_i Q_i^2 c_i[1-\frac{I(x_i)}{x_i}],
\end{aligned} \tag{A5}$$

where $k_{1,2}$ and $\epsilon_{1,2}$ are the momenta and polarization of the two photons, with $(k_1 k_2)$ the dot product given by a metric with signature $(1,-1,-1,-1)$. The sum runs over the fermions exchanged in the loop and here $x_i^2 = (k_1+k_2)^2/(4m_i^2)$. All other symbols were defined in Sec. II. From the above effective interactions and Feynman rules one can easily derive the cross sections to leading order in $1/M_{\tilde{f}}^2$ or $1/m_W^2$ as presented in Sec. II. In the case of the loop of $W^\pm$ and charginos, the validity of the effective interaction procedure can be checked by working in the unitary gauge and retaining only the leading terms of the the $W^\pm$ propagator.

REFERENCES

1. For a general review and list of references see J. R. Primack, D. Seckel and B. Sadoulet, *Ann. Rev. Nucl. Part. Sci.* **38** (1988) 751.
2. L. Bergström and H. Snellman, *Phys. Rev.* **D37** (1988) 3737; L. Bergström, University of Stockholm preprint USITP-88-12 (1988); L. Bergström, University of Stockholm preprint USITP-89-01 (1989).
3. The Gamma-Ray Observatory Science Plan, D. Kniffen, chairman (1988).
4. ASTROGAM, Volume I, Investigation and Technical Plan, J. H. Adams, Jr., Principal Investigator, Naval Research Laboratory preprint, 1989.
5. M. Srednicki, S. Theisen, and J. Silk, *Phys. Rev. Lett.* **56** (1986) 236; **56** (1986) 1883(E); S. Rudaz, *Phys. Rev. Lett.* **56** (1986) 2128.
6. S. Rudaz, University of Minnesota preprint UMN-TH-716/89 (1989).
7. A. Bouquet, P. Salati, and J. Silk, LBL preprint LBL-26749 (1989).
8. S. Raby and G. West, *Nucl. Phys.* **B292** (1987) 793; S. Raby and G. West, *Phys. Lett.* **194B** (1987) 557.
9. H. E. Haber and G. L. Kane, *Phys. Rep.* **117** (1985) 75.
10. J. Ellis, J. S. Hagelin, D. V. Nanopoulos, K. A. Olive and M. Srednicki, *Nucl. Phys.* **B238** (1984) 453.
11. K. Griest, *Phys. Rev.* **D38** (1988) 2357.
12. R. Barbieri, M. Frigeni, and G. F. Giudice, *Nucl. Phys.* **B313** (1989) 725.
13. J. F. Gunion and H. E. Haber, *Nucl. Phys.* **B272** (1986) 1.
14. M. S. Turner, *Phys. Rev.* **D34** (1986) 1921.
15. J. Ellis, K. Freese, S. Ritz, D. Seckel, and J. Silk, *Phys. Lett.* **B214** (1988) 403.
16. One expects large mass splittings in models where the scalar colored particles acquire large radiative corrections to their masses due to the strong interaction. Assuming a gaugino mass unification relation, one finds $M_{\tilde{e}} \approx (g_2^2/g_3^2)M_{\tilde{q}} \approx M_{\tilde{q}}/3$, where g_2 and g_3 are the weak and strong coupling constants. By displaying results for both the degenerate and non-degenerate cases we hope to bracket commonly considered supersymmetry models.

17. K. Griest and D. Seckel, *Nucl. Phys.* **B283** (1987) 681; (E) **B296** (1988) 1034.

18. F. W. Stecker and A. J. Tylka, preprint, to appear in *Astrophys. J.* Aug. 1989.

19. F. Abe, *et al.* (CDF collaboration), *Phys. Rev. Lett.* **62** (1989) 1825.

20. C. Hearty *et al.*, *Phys. Rev. Lett.* **58** (1987) 1711; G. Bartha *et al.*, *Phys. Rev. Lett.* **56** (1986) 685.

21. I. Adachi, *et al.* (TOPAZ collaboration), *Phys. Lett.* **218B** (1989) 105.

22. D. P. Stoker, *et al.*, *Phys. Rev.* **D39,** (1989) 181.

23. J. R. Ipser and P. Sikivie, *Phys. Rev.* **D35** (1987) 3695.

Figure Captions

1. Feynman diagrams contributing to neutralino ($\widetilde{\chi}$) annihilation into two photons (γ). Additional diagrams with exchanged neutralino and photon external legs are not shown. The symbol $\tilde{f}$ stands for either a left or right chiral sfermion (squark or slepton) and f for a left or right chiral fermion (quark or lepton).

2. Feynman diagram for Z^0 exchange contribution to neutralino annihilation into two photons. The diagram with exchanged photon legs is not shown.

3. Constraints on sfermion (squark and slepton) masses from relic abundance and particle accelerator experiments. As a function of the photino mass (m_γ), the masses of the squarks (solid lines) and selectrons (short-dash line) required to give the indicated value of $\Omega_{\tilde{\gamma}}h^2$ are shown. Fig. 3a is for $\Omega_{\tilde{\gamma}}h^2 = .25$ and Fig. 3b for $\Omega_{\tilde{\gamma}}h^2 = .025$. Both the split ($M_{\tilde{e}} = M_{\tilde{q}}/3$) and not split ($M_{\tilde{e}} = M_{\tilde{q}}$) cases are shown. One long-dash line shows the CDF lower limit on squark masses, while the other shows the ASP limit on the selectron mass. Regions below these lines are ruled out.

4. Predicted counting rate of photons in the ASTROGAM detector from annihilation of galactic photinos as a function of the photino mass. The sfermion masses were found by requiring $\Omega_{\tilde{\gamma}}h^2 = .25$ (4a) or $\Omega_{\tilde{\gamma}}h^2 = .025$ (4b) (see Fig. 3). Both the split ($M_{\tilde{e}} = M_{\tilde{q}}/3$, short-dash line) and the not split ($M_{\tilde{e}} = M_{\tilde{q}}$, solid line) cases are shown, as is a background counting rate estimate of Stecker and Tylka (long-dash). See Sec. III for more details.

5. Same as fig. 4 for the GRO EGRET device.

6. Photon counting rate for ASTROGAM detector from general neutralino annihilation. Chargino exchange is included and all points satisfy $\Omega_{\tilde{\chi}} h^2 = .025$. See Sec. III for more details.

7. Feynman diagram contributing to luxino (l^0) annihilation into two photons. The diagram with exchanged photons is not shown.

8. Feynman diagram for effective interaction of neutralinos and photons.

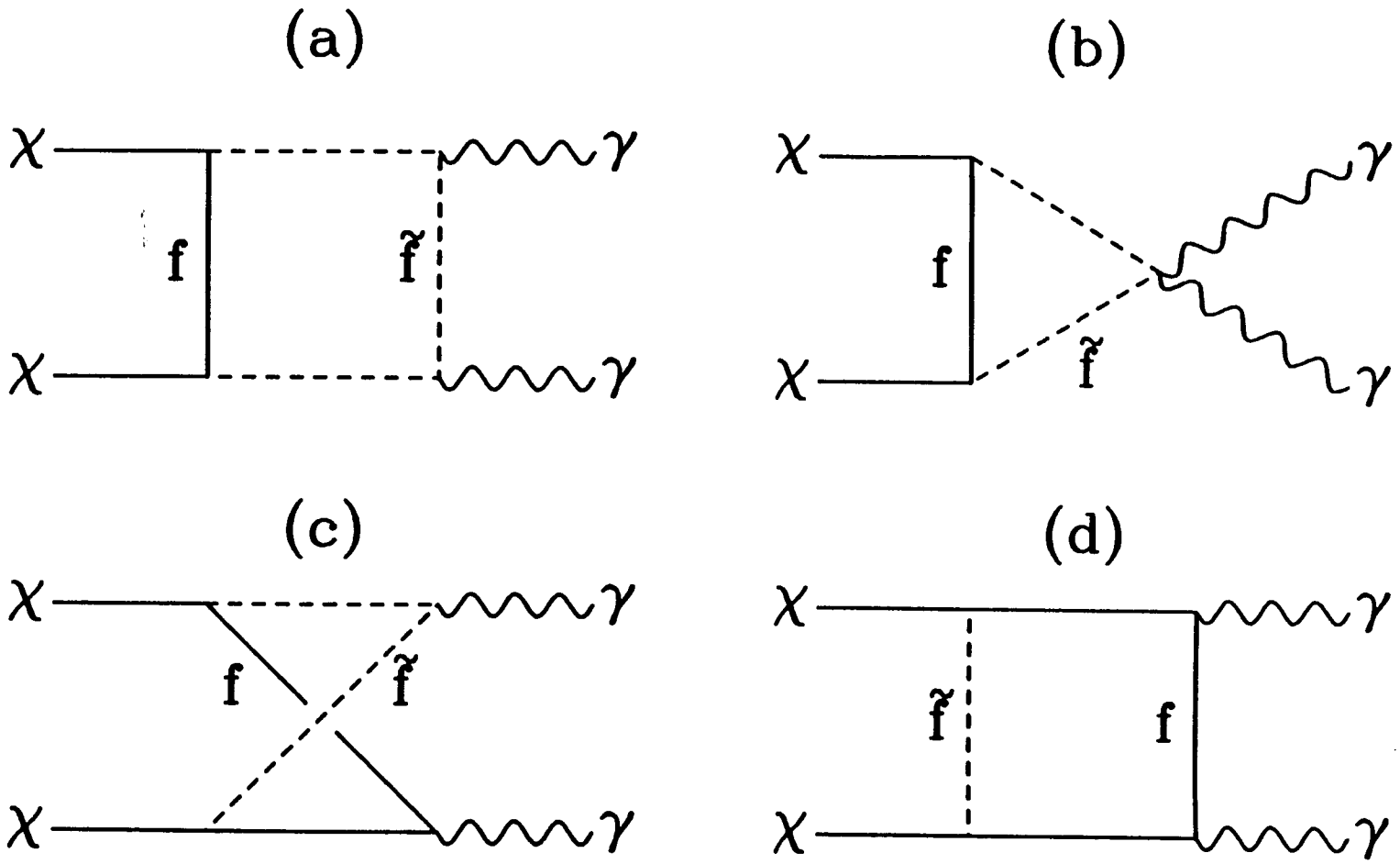

Fig 1

GIUDICE 8

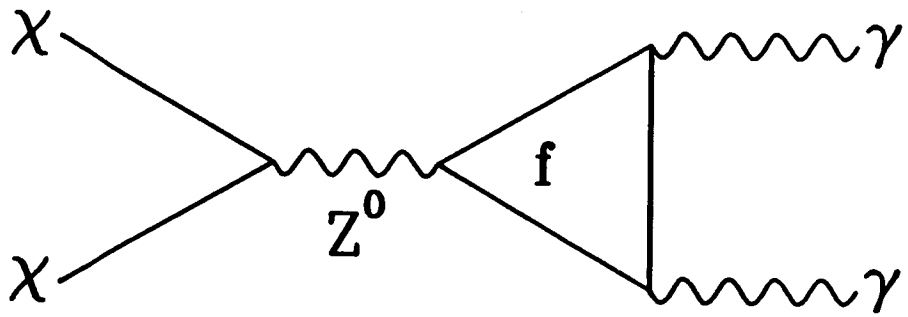

Fig 2.

GIUDICE & GRISST

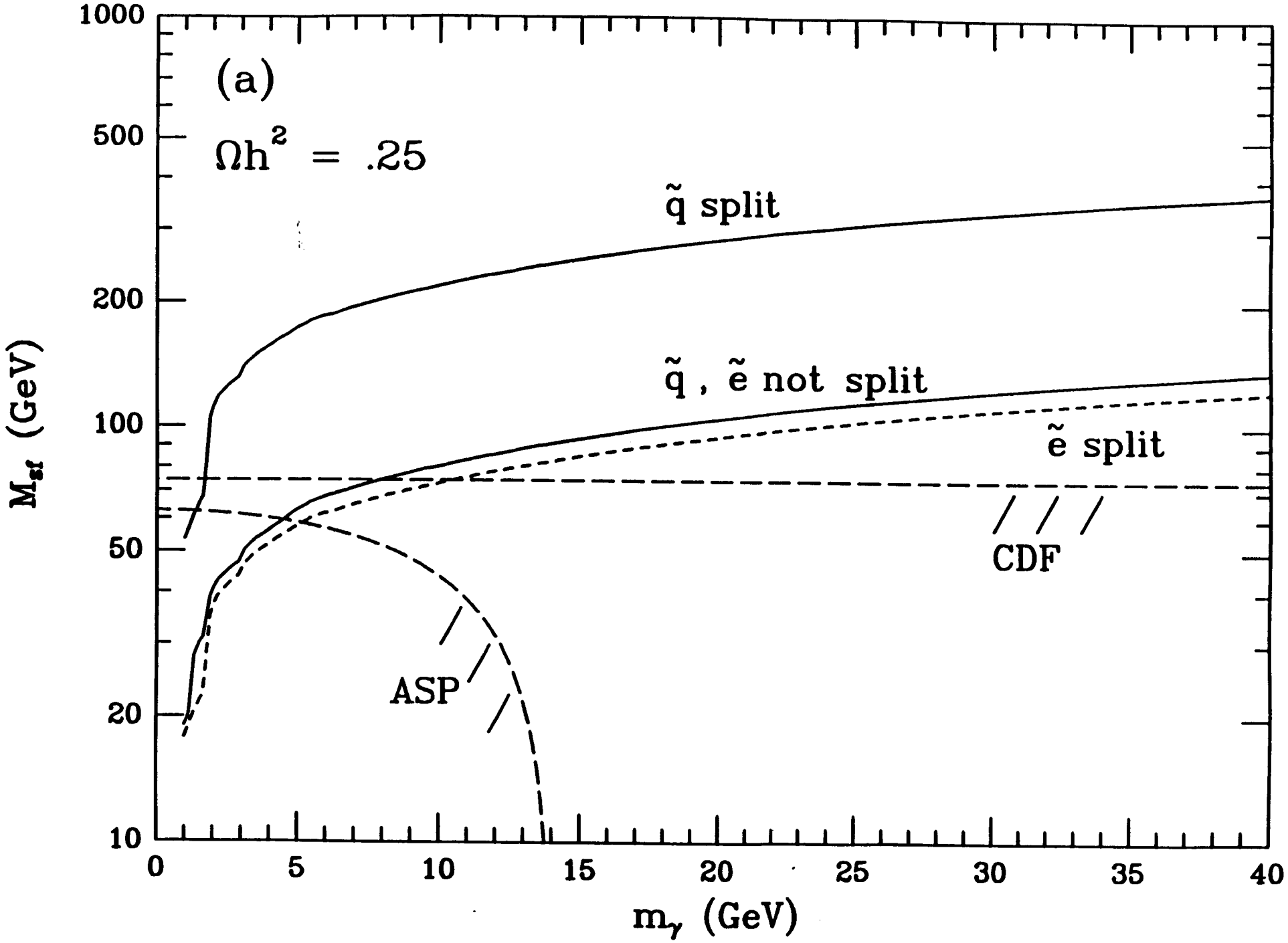

Fig 39

GIUDICE & GRIEST

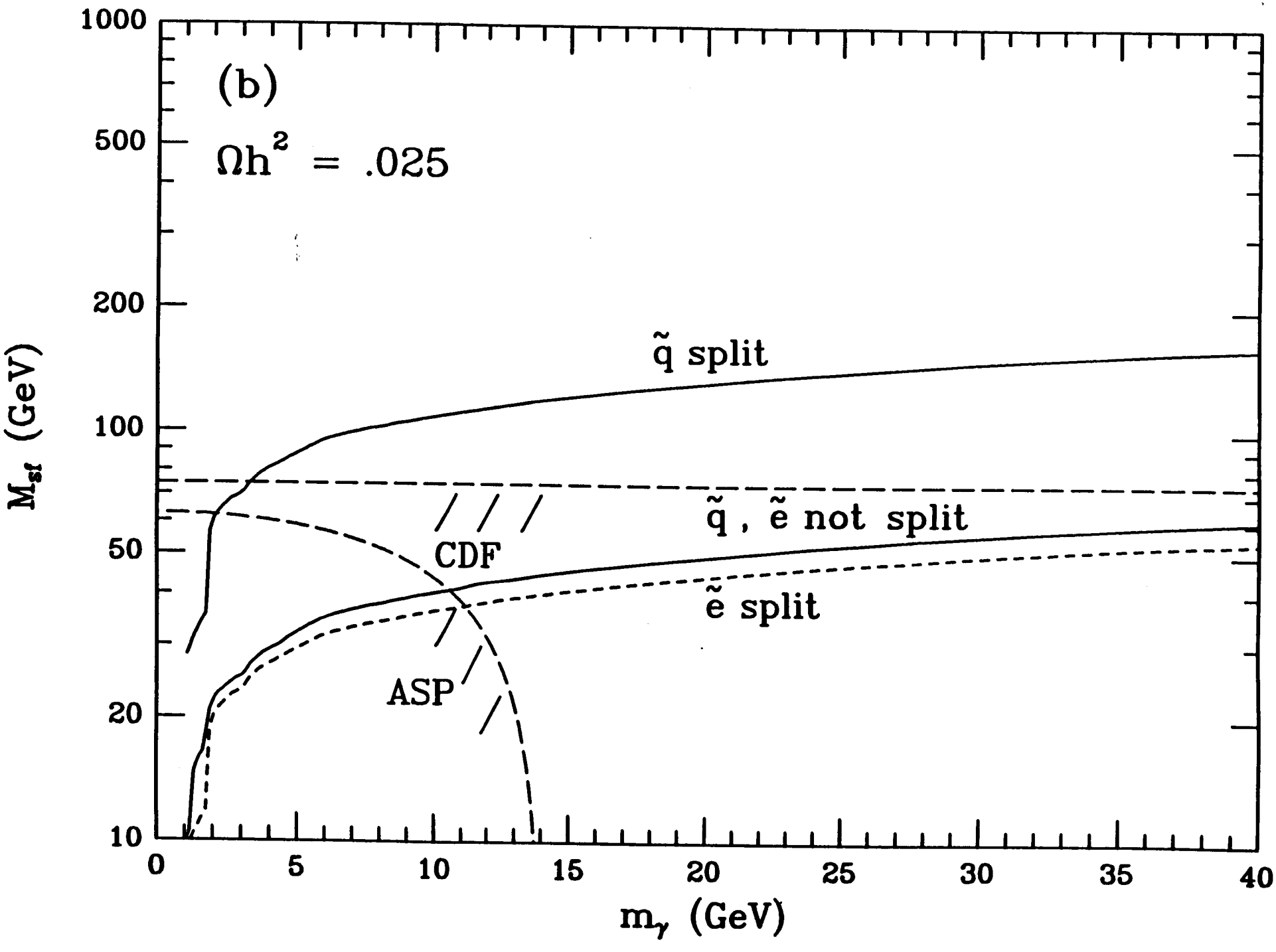

Fig 3b

GIUDICE & GRIEST
Fig 3b

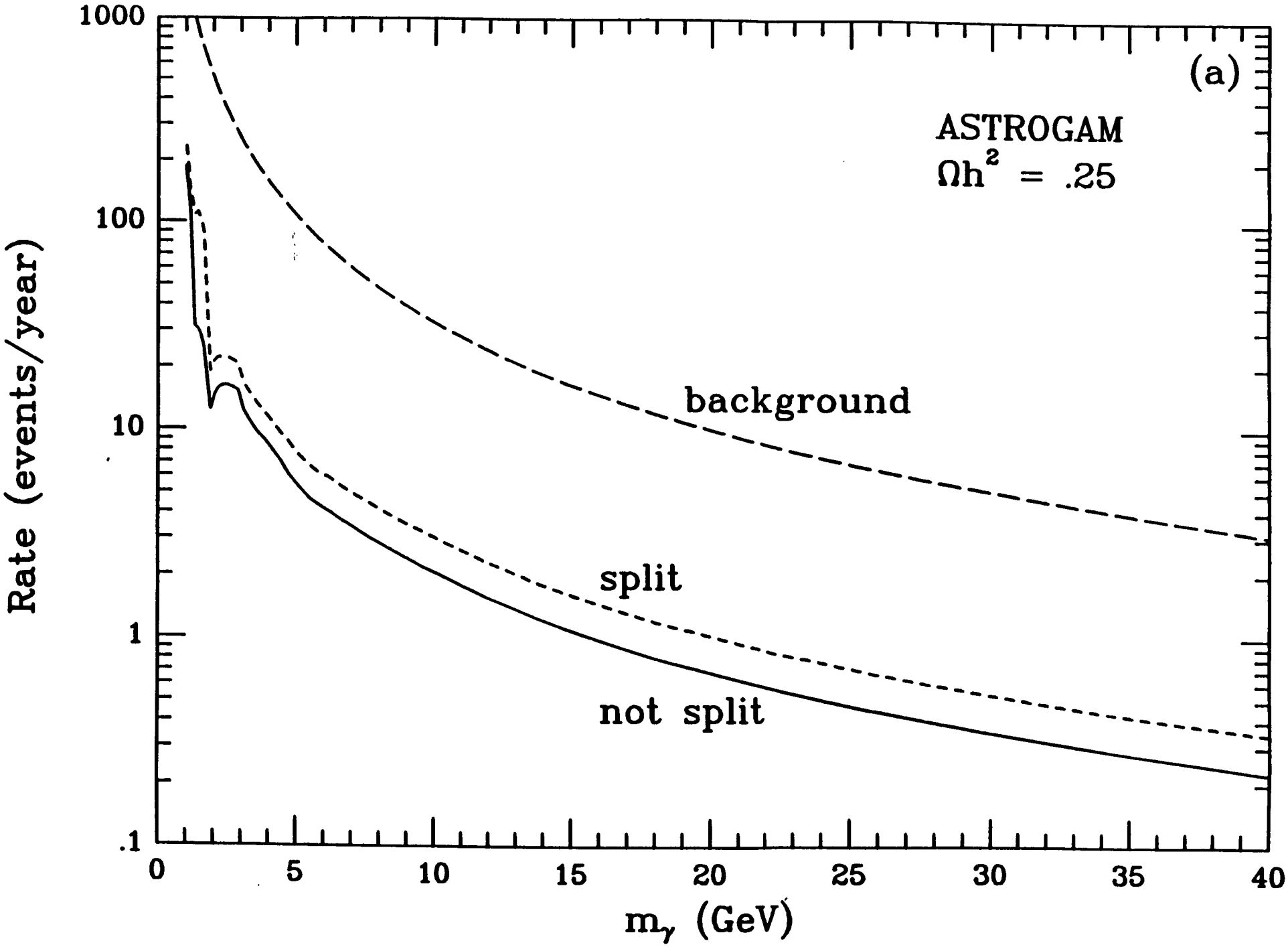

Fig 49

GIUDICE & GRIEST

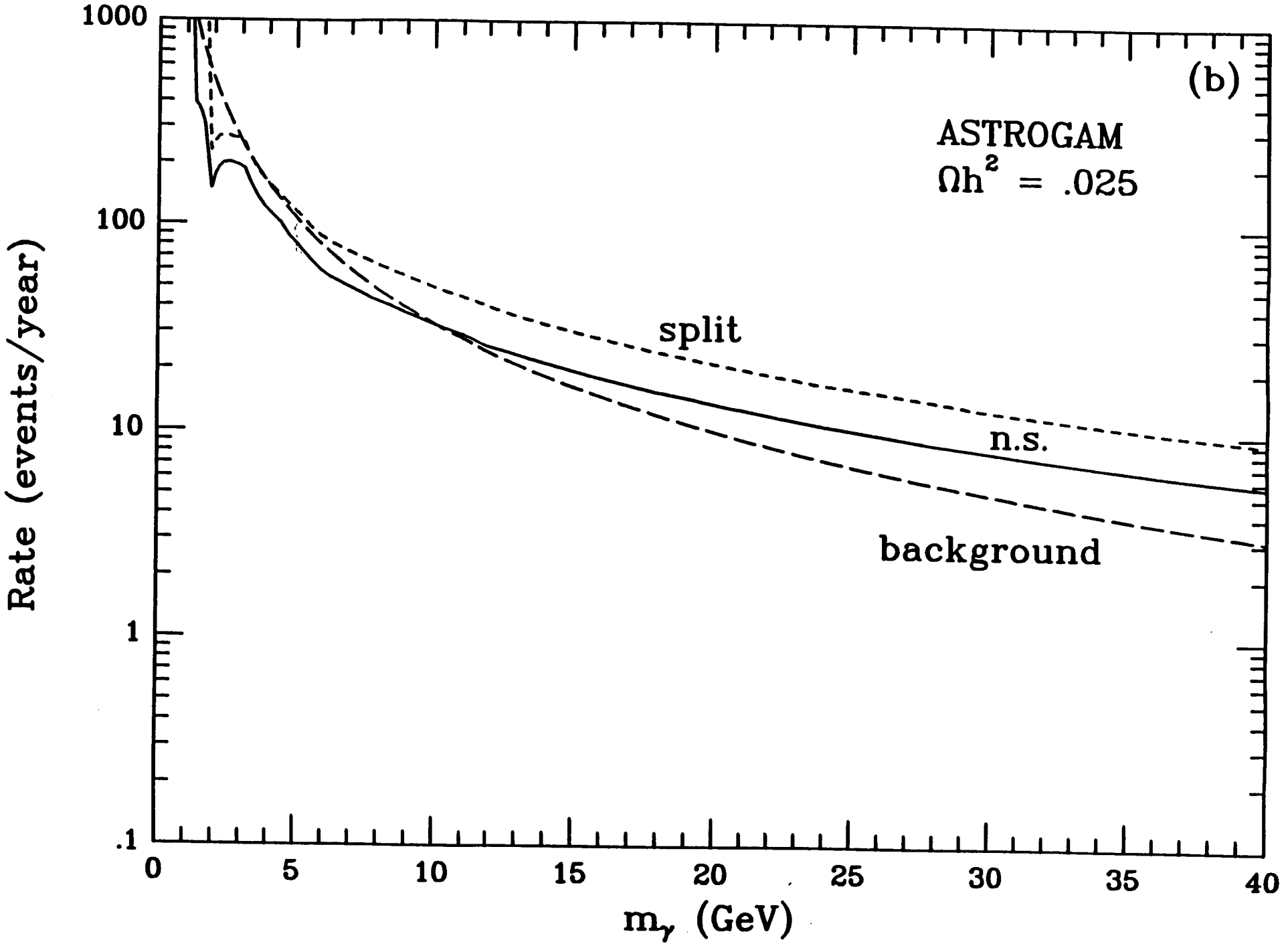

Fig 4b

GIUDICE & GRIEST

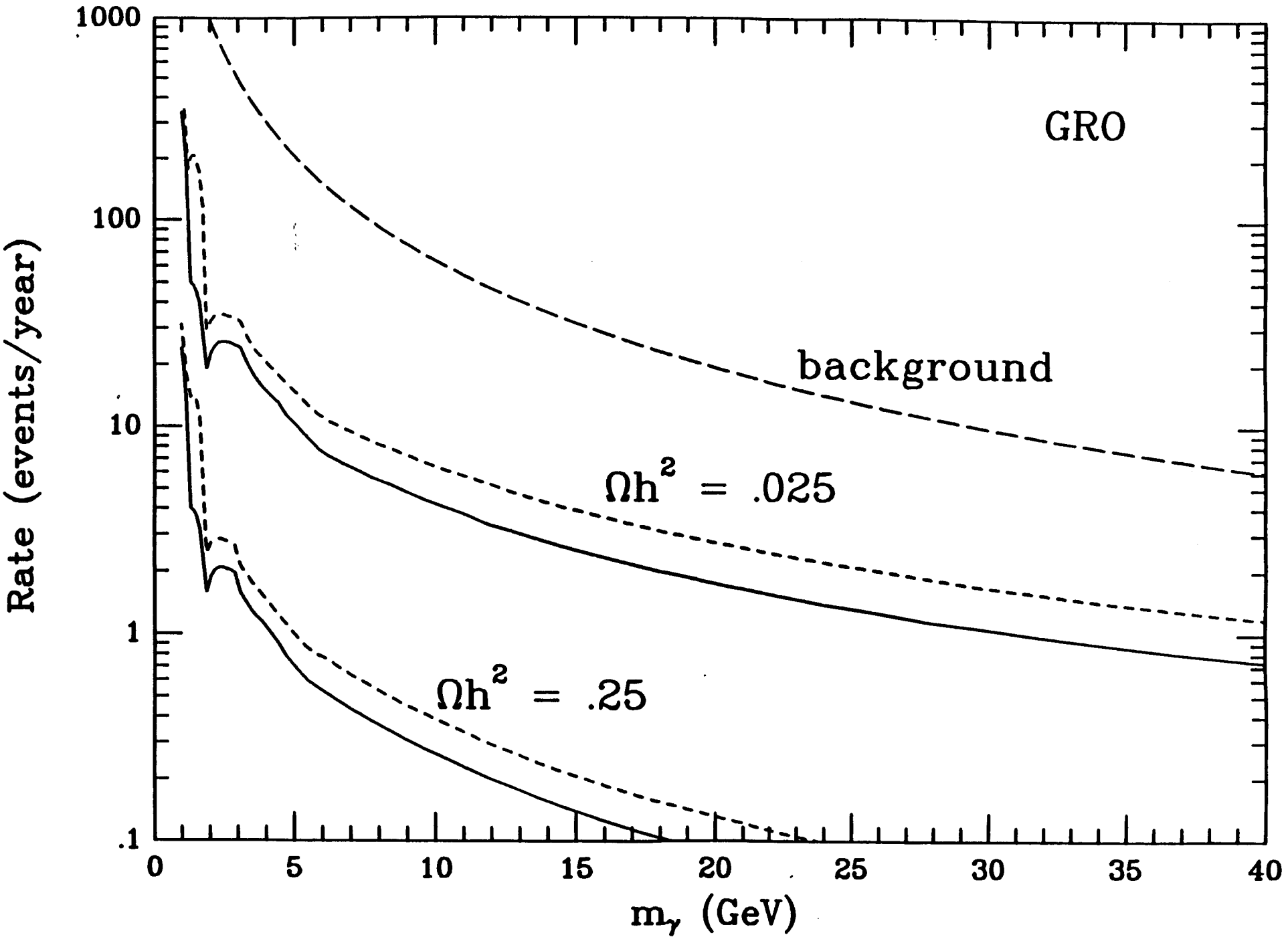

Fig 5

GIUDICE & GRUSE

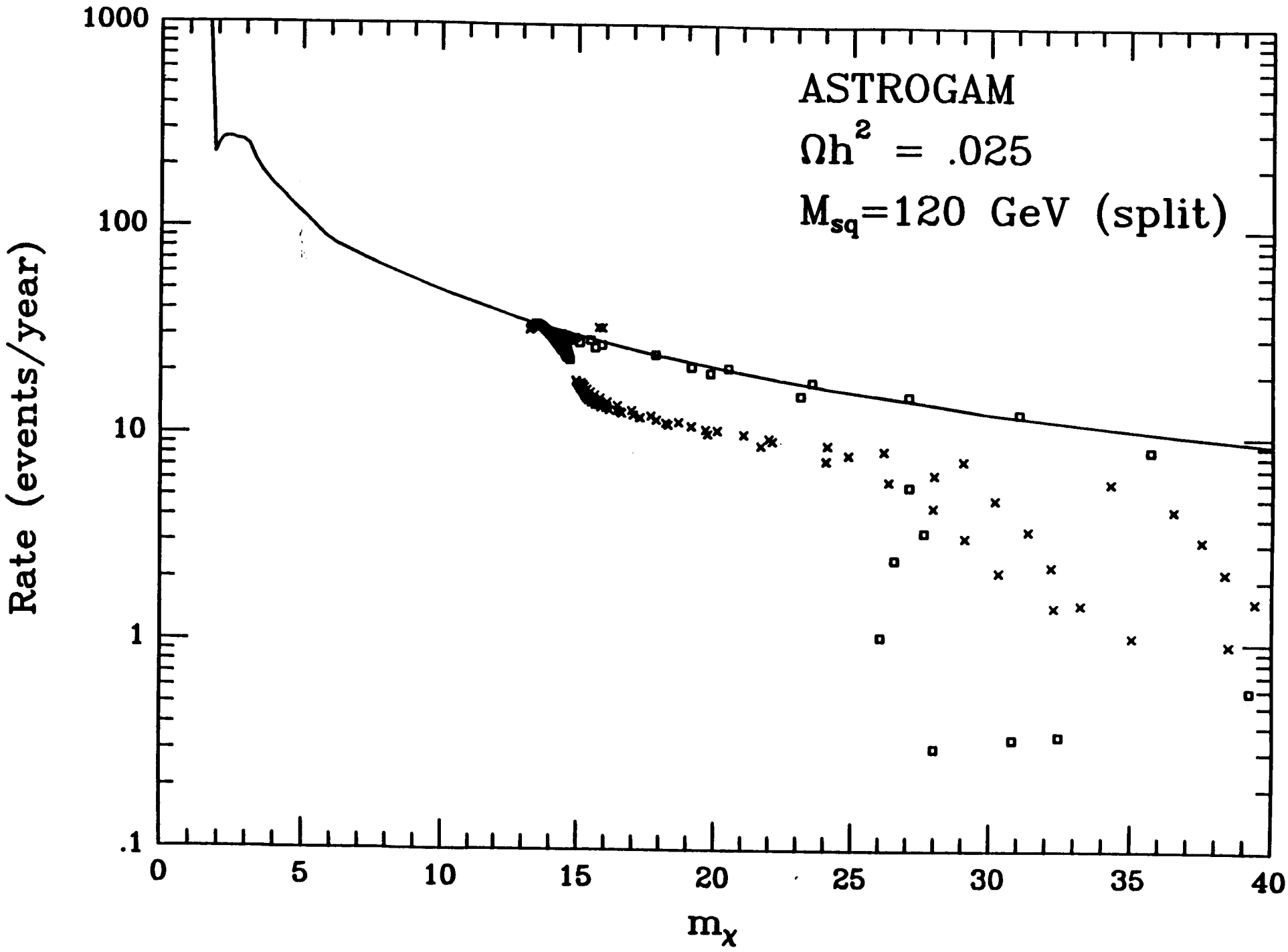

Fig. 6

GIUDICE & GRIFST

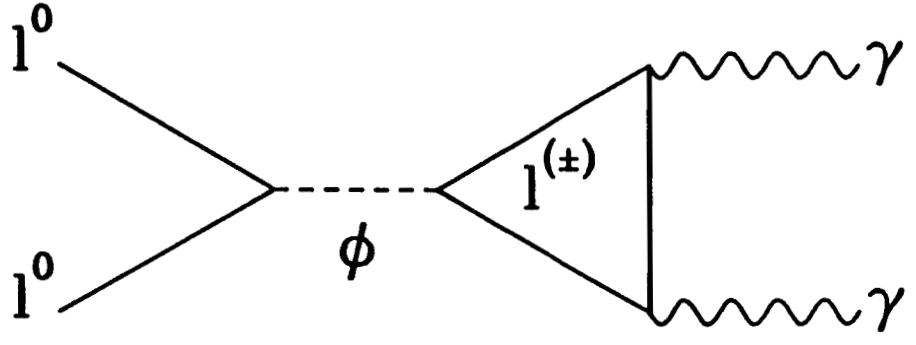

Fig. 7

GIUDICE & -

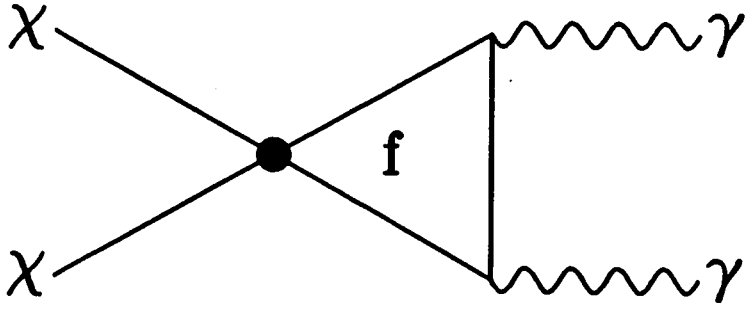

Fig 8

GIUDICE & GRIEST